Surface plasmon resonance response of Au–WO3−x composite films

Chen, Bo; Yang, Dongfang; Lin, Chii-Wann

Publisher's version / Version de l'éditeur:
https://doi.org/10.1007/s00339-009-5249-4
Applied Physics A, 97, 2, pp. 489-496, 2009-11-01

Surface Plasmon Resonance Response of Au-WO_{3-x} Composite Films

Bo Chen[a], Dongfang Yang[a,*] and Chii-Wann Lin[b]

a) Industrial Materials Institute, National Research Council, 800 Collip Circle, London, Ontario, Canada N6G 4X8

b) Medical Micro-sensor and System Laboratory, Institute of Biomedical Engineering and Department of Electrical Engineering, National Taiwan University, Taipei, Taiwan, R.O.C.

Abstract

Surface plasmon resonance (SPR) of metal-dielectric composite thin films formed by noble metal nanoparticles embedded in a dielectric matrix offers a high degree of flexibility and enables many applications such as surface enhanced spectroscopes, and biological and chemical sensing. In this article, Au-WO_{3-x} composite films of various Au content and thickness were prepared by the pulsed laser deposition technique, their SPR responses were investigated for various Au percentage and film thickness in the Kreschmann geometry. Theoretical calculation of SPR responses based on Bruggeman or Maxwell-Garnett model with the MacLeod general characteristic matrix method is obvious discrepancy with experimental measurements but it is able to predict the trend in term of the dependence of SPR responses on Au content and thickness of the Au-WO_{3-x} films.

PACS 73.20.Mf; 81.07.-b; 78.66.-w; 81.15.Fg

[*]Corresponding author. Tel.: +1-519-430-7147; Fax: +1-519-430-7064.
E-mail address: Dongfang.Yang@nrc.gc.ca (Dongfang Yang).

1. Introduction

Materials that possess a large negative real and small positive imaginary dielectric constant are capable of supporting a surface plasmon wave, which can be excited in a resonant manner by a visible or infrared light beam from a glass prism in either Otto [1] or Kretschmann [2] configurations. The materials used for supporting surface plasmon waves must have free conduction band electrons capable of resonating with the incoming light at a suitable wavelength. Typically, thin noble metal films (~50 nm) such as Gold (Au) and Silver (Ag) are commonly used as the platform for supporting the surface plasmon waves, other metals are either too reactive or too expensive or too susceptible to oxidation. Surface plasmon resonance (SPR) phenomena at the metal/dielectric interface have enabled a vast array of applications such as surface enhanced spectroscopes [3], and biological and chemical sensing [4, 5].

Nanocomposite [6] thin films formed by noble metal nanoparticles embedded in a dielectric matrix can also show SPR response when irradiating by e.g. a laser light due to collective excitations of conduction electrons in metal nanoparticles when photons are coupled to the metal particle–dielectric interface. The microstructures of metal-dielectric composites can be classified roughly into two types, the separated-grain structure in which the metal particles are dispersed in a continuous host of dielectric medium, and the aggregate structure in which constitutes metal and dielectric particles mix randomly to form a space-filling mixture. Maxwell-Garnett effective medium theory was developed for the optical property analysis of the separated-grain structure, while Bruggeman theory was developed for the aggregated structure [7].

If a composite material is composed of two mediums with dielectric constant ε_1 and ε_2, respectively, and the volume filling factor of medium 1 is f_1, then the effective permittivity of the composite calculated from Maxwell-Garnett theory for the separated-grain structure is:

$$\varepsilon_{eff} = \varepsilon_2 \frac{\varepsilon_1 + 2\varepsilon_2 + 2f_1(\varepsilon_1 - \varepsilon_2)}{\varepsilon_1 + 2\varepsilon_2 - f_1(\varepsilon_1 - \varepsilon_2)} \qquad (1)$$

and the effective permittivity of the composite calculated from Bruggeman theory for the aggregated-grain structure is:

$$f_1 \frac{\varepsilon_1 - \varepsilon_{eff}}{\varepsilon_1 + 2\varepsilon_{eff}} + (1 - f_1)\frac{\varepsilon_2 - \varepsilon_{eff}}{\varepsilon_2 + 2\varepsilon_{eff}} = 0 \qquad (2)$$

When using a visible or infrared light beam to excite surface plasma waves in the Kretschmann configuration, the light is shone on the wall of a prism and totally reflected. An evanescent wave penetrates through the metal-dielectric composite film that is evaporated onto the prism to excite and interact with the plasma waves at the metal particle-dielectric interface. Under certain conditions, free electrons respond collectively by oscillating in resonance with the incident light wave to generate surface plasmon resonance (SPR). The SPR response is generally characterized by the reflectance of the p-polarized incident beam, i.e., Rp , which can be calculated as [8], [9]

$$R_p = \left| \frac{r_{pm} + r_{md}\exp(2ik_{zm}d_m)}{1 + r_{pm}r_{md}\exp(2ik_{zm}d_m)} \right|^2 \qquad (3)$$

with $r_{pm} = \frac{\varepsilon_p k_{zm} - \varepsilon_m k_{zp}}{\varepsilon_p k_{zm} + \varepsilon_m k_{zp}}$ and $r_{md} = \frac{\varepsilon_m k_{zd} - \varepsilon_d k_{zm}}{\varepsilon_m k_{zd} + \varepsilon_d k_{zm}}$. Here k is the wavenumber, d is the film thickness, and $i = \sqrt{-1}$ is the imaginary symbol. The wavenumbers along x- and z- directions are

$k_x = n_p k_0 \sin\theta_p$ and $k_{zi} = \sqrt{\varepsilon_i k_0^2 - k_x^2}$, respectively. The subscripts *0*, *p*, *m*, and *d* denote free-space, prism, metal, and dielectric (ambient or embedding material), respectively.

The reflectance can also be obtained from Macleod's general characteristic matrices method [10] :

$$R = \left(\frac{\eta_g - Y}{\eta_g + Y}\right)\left(\frac{\eta_g - Y}{\eta_g + Y}\right)^* \quad \text{with } Y = \frac{C}{B} \tag{4}$$

where
$$\begin{bmatrix} B \\ C \end{bmatrix} = \begin{bmatrix} \cos\delta_c & (i\sin\delta_c)/\eta_c \\ i\eta_c \sin\delta_c & \cos\delta_c \end{bmatrix} \begin{bmatrix} 1 \\ \eta_0 \end{bmatrix} \tag{3}$$

Here η_i is the optical admittance, and $\delta = 2\pi N_i d_i / \lambda$, d_i is the thickness of the composite film and λ is the wavelength. The subscripts *0*, *c*, and *g* represent air, composite layer, and the glass substrate, respectively.

Randomly inhomogeneous composite materials have unusual properties, which are absent in bulk materials. To explain optical properties of such inhomogeneous materials with a simple effective dielectric constant calculated with effective-medium theories is expected to be rather limited. Maxwell-Garnett and Bruggeman theories have only been applied for inhomogeneous media composed of spherical particles, which may not be able to account for other particle shapes such as medium composed of randomly oriented ellipsoidal particles. There are needs for direct experimental results to test those effective-medium theories. SPR response of metal-dielectric composite films prepared by physical vapor deposition methods such as pulsed laser deposition (PLD) offers the best model system for such purpose. The aim of this work is to study the SPR response of Au-WO_{3-x} composite [6, 11] films fabricated by PLD method, to observe its evolution with varying Au content and thickness, and to compare the theoretical simulation with experimental measurement. Tungsten oxide (WO_{3-x}) was selected as the dielectric material [11, 12] due to its interesting gas sensing property, while Au was selected as the metal to carry the SP waves as it is the most common materials used for the SPR [13]. Simulation of the SPR response of Au–WO_{3-x} films will be done using Macleod's general characteristic matrices method in the Kretschmann configuration with 632.8nm laser light excitation. The dielectric constants of Au-WO_{3-x} composite thin films will be determined using either Maxwell-Garnett or Bruggeman effective medium theory. Experimental SPR responses of the Au-WO_{3-x} composite films will be determined using a light emitting diode at the wavelength of ~ 640 nm in the Kretschmann configuration for various film thicknesses and metal volume fractions. Experimental data will be compared with simulation results to exam the applicable range of the theories.

2. Experimental Details

For the composite film deposition experiments, a pulsed laser beam generated by a KrF excimer laser at a wavelength of 248 nm and pulse duration of 25 ns was introduced into the deposition chamber through a quartz window, and focused with optical lenses onto an Au/WO_3 target surface [14]. The Au/WO_3 target was prepared in the following way: first, a 3-inch circular Tungsten oxide (WO_3) target dish was cut into pie-shaped pieces with different angles, then a WO_3 target piece of selected angle was mounted on the top of a 3-inch circular Au target dish. The laser beam was subsequently ablated on the rotating WO_3/Au targets at a speed of 18 rpm to form composite thin films deposited directly on the 18 mm x 18 mm x 1.0 mm BK7 glass substrates or a piece of silicon wafers. The laser fluence on the target was 2 ~ 3 J/cm^2, while the repetition rate was fixed at 50 Hz. To improve the film homogeneities, the substrates were rotated along the vertical axis at a speed of 35 rpm. Films were deposited at 20 °C or 500 °C substrate temperatures under high vacuum with base pressure of 2.0 x 10^{-6} Torr or lower.

The SPR responses were measured by a Biosuplar 6.0 built in the Kreschmann geometry with a retro-reflecting measurement prism installed on a rotating table. During the device operation, the back side of the BK7 substrate was glued onto the top face of the prism using immersion liquids and the Au-WO_{3-x} film coated side was faced to ambient directly. To measure the SPR response, a transverse magnetic (TM) polarized light (~ 640nm) generated from a light emitting diode was used to irradiate the Au-WO_{3-x} film and the reflected light were monitored as the function of incident angle. The cross-sectional images of the films taken by a Leo 440 field emission scanning electron microscope (FE-SEM) were analyzed for the estimation of film thickness, while the compositions of the films were investigated by x-ray photoelectron spectroscopy (XPS). The XPS measurements were performed using a spectrometer equipped with an Al$K\alpha$ source (λ = 1486.6 eV). The crystallographic properties of the composite films were analyzed by X-ray diffraction (XRD) using a diffractometer, arranged in an upper beam set-up. The incident angle of the X-ray beam was fixed at 0.5° for all measurements. The diffraction photons were collected by the diffractometer from 20-70° with a 0.02° step size, employing a Cu-$K\alpha$ radiation.

3. Results and Discussions

SPR responses of Au-WO_{3-x} films on BK7 substrates with various Au content are shown in Figure 1. The volume fraction (f_1) of Au of the films is varied from 100 to 75 %. The thicknesses of both pure WO_{3-x} and Au films deposited on silicon wafer by PLD were measured by the FE-SEM first. From the thicknesses and deposition times, the ratio of the deposition rates of WO_{3-x}

and Au ($R_{dr}(WO_{3-x}/Au)$) was determined to be 3.74. Then, the f_l of Au in the composite films was obtained from the ratio of the angles of WO_3 and Au target pie-shaped pieces ($R_{angle}(WO_{3-x}/Au)$) through $f_1 = 1/[1 + R_{dr}(WO_{3-x}/Au) \times R_{angle}(WO_{3-x}/Au)]$. The f_l values for the films were used for the theoretical calculation of the SPR responses, as described previously in equation 1 and 2. The index of refraction, n, and extinction coefficient, k, used in the calculation of dielectric constant of Au were obtained from the CRC Handbook of Chemistry and Physics [8], and other literatures [9, 15, 16, 17]. The refractive index n and extinction coefficient k for Au were found to be n = 0.16172 and k = 3.21182 at the wavelength of 632.8 nm (1.9593 eV) (i.e. the wavelength of He-Ne laser). The n and k values of Au-WO_{3-x} composite films used in the calculation of dielectric constant of WO_{3-x} films were measured from WO_{3-x} films deposited by the PLD. The WO_{3-x} films were deposited by ablating a 90 mm diameter rotating WO_3 (99.99% purity, from Super Conductor Materials) in high vacuum (< 10^{-6} torr) at 20°C. The resulting films are non-stoichiometric with oxygen deficiency (e.g., WO_{3-x}, where x > 0). The optical reflectance spectra of WO_{3-x} films were measured with a fiber-optic-based spectrophotometer (SCI Film TEK3000). Their n and k values were calculated from the reflectance spectra by using appropriate material model to fit the measurement data and the n and k values for WO_{3-x} films were determined to be 2.637 and 0.909, respectively, at the wavelength of 632.8 nm. The n, k values of Au and WO_{3-x} were then used to calculate the effective dielectric constants of Au-WO_{3-x} composites films. After the dielectric constants were determined, the SPR response of Au-WO_{3-x} composite films was calculated using Macleod's general characteristic matrices method at 632.8 nm in the Kretschmann configuration. The thickness of Au-WO_{3-x} composite films presented in Figure 1 corresponds to 44, 28, 36, and 32 nm respectively. The solid and dashed curves represent the experimental and simulated data (only show results calculated by Bruggeman model), respectively.

Clearly, when the Au metal percentages in the composite films decreases, the reflectance minimum of shifts to higher values of incident angle and the width of SPR dip becomes broader as shown in both theoretical calculations and experimental measurements in Figure 1. The width of the SPR response is strongly related to the ratio of the extinction coefficient and refractive index (k/n) of the SPW supporting material. Generally, the larger the ratio, the narrower the width if the thickness of the SPW supporting layer is optimized. The n and k values of Au were 0.1617 and 3.2118, respectively, at the wavelength of 632.8 nm, while the n and k of WO_{3-x} was measured to be 2.637 and 0.909, respectively. The optical property of the Au-WO_{3-x} composite is basically a combination of that of constituent materials; therefore, the values of n and k of the composite should be in between the values of the two materials. As the Au volume percentage decreases, the refractive index of the composites increases while the extinction coefficient decreases as predicted by the Bruggeman model. Therefore, the ratio of k/n becomes smaller as the Au percentages decreases, resulting in broader SPR responses. The reflectance almost approaches zero at the angle of incidence of 43.6° for the 42 nm pure Au film. The SPR response of the pure Au film fabricated by PLD is very close to that of a commercial pure Au films prepared by the sputtering technique. As the Au percentage decreases to 77%, the minimum of the SPR response is hardly to be distinguishable. Therefore, only the films with relatively higher Au volume percentages will give out a sharp SPR dip which is important for biological and chemical SPR sensing since typically the detection angle is fixed at the dip to achieve the best sensitivity. If dielectric portion of the composite film is the crucial component for the SPR sensing, too low dielectric percentages may not be desirable [18]. There may be a trade off between the sharp SPR dip and its sensing sensitivity. Although there is obvious difference between the reflectance values of the solid and dashed curves, the theoretical calculations have the similar trend as the experimental data in term of their dependence on the Au percentage and film thickness.

Figure 2 shows the SPR responses of various thickness Au-WO_{3-x} composite films with 88 volume % Au. The solid and dashed curves correspond to the experimental and theoretical results (only shown results from Bruggeman model), respectively. For the 20nm film, the reflectance approaches zero at around 45.5 degree of incident angle. The minimum reflectance of thicker films (e.g. 45nm and 65nm) is larger and do not achieve zero at any incident angle. The SPR dip of the 45nm film is sharpest but its reflectance values are larger that that of 20nm film. Although there are some obviously difference between the theoretical and experimental results, they have the similar trend in term of their dependence on the Au percentage and film thickness as well. The theoretical calculation may not be able to give exact values on the SPR response, but it helps to predict the optimized conditions (i.e. metal percentage and film thickness) for the best SPR shape needed for sensing purpose.

Calculations of the optical properties (i.e. n and k) of the Au-WO_{3-x} composite films were also carried out using Maxwell-Garnett effective medium theory in order to compare with Bruggeman theory and the experimental results. Figure 3 shows experimental results and simulated data using both theories for a 32 nm and a 45 nm Au-WO_{3-x} films with 91 volume% Au. It is clear that SPR responses calculated from either Maxwell-Garnett or Bruggeman theory with the Macleod's method do not agree well with that of experimental date indicating that both theories may be too simplify to describe the complex metal-dielectric composites deposited by the PLD. The PLD composite films can neither be described as a separated-grain structure

(Maxwell-Garnett) or an aggregated structure (Bruggeman). The experimental data are sitting in between the two simulated results indicating that the structure of the PLD composite films is complicated and may not be described simply as separated-grain or aggregated-grain structures. However, the shape of SPR response predicted by Bruggeman model is closer to experimental results indicating that the PLD films could be characterized more closely as the aggregated-grain structure than separated-grain structure. More sophisticated effective medium theories should be used or developed to interpreter the experimental data.

Figure 4 shows the SPR responses of Au-WO_{3-x} composite films of 88 volume % Au that were deposited at 20°C (dashed curves) and 500°C (solid curves), respectively. The insets show the microstructures of both films taking by FE-SEM. The incident angles at the reflectance minima of the two films are quite different, i.e. 8 degree, and the width of the SPR dip of the film deposited at 500°C is much broader than that at 20°C. Although small thickness variation may be contributed to this difference, the main reason for this is the microstructure difference. Visually, the SEM pictures showed very different microstructures for the two films. The 20°C film is very smooth and consists of very fine grains, while the 500°C film consists of many large grains with ~ 60 nm grain size.

To further analyze the microstructures of the two films, the XRD patterns for both films were recorded and the results are shown in Figure 5. Both composite films (having a thickness of 30 nm) showed XRD peaks at angles of 38.22°, 44.43° and 64.64°, with no substrate peaks being observed. These peaks can be indexed as the diffractions from the (1 1 1), (2 0 0) and (2 2 0) planes of cubic Au [JCPDS 04-0784]. No peaks were observed in the XRD patterns that are originated from the WO_{3-x}, which means only amorphous structure WO_{3-x} is present in both films. The results clearly illustrate that Au is crystallized in the Au-WO_{3-x} composite films while

WO_{3-x} existed as an amorphous structure. All the three Au peaks for 20°C film are weak and broad, which indicates that the Au grain size is very small which is consisting with the SEM image in the inset of Figure 4. The appearance of dual-peak may be contributed by two types of Au particles with different lattice constants co-existing in the composite films. Very likely, the dual peak originates from the Au nanoparticles in the composite film and micro or sub-micron sized Au particles embedded in the composite films. Those micro or sub-micron sized Au particles were generated during the pulsed laser ablation process [19]. The three Au peaks for 500°C film, however, are much more intensive than that of 20° film, indicating that the grain size of the Au-WO_{3-x} film is much bigger. This again is consisting with SEM image in the inset of Figure 4.

The experimental SPR responses of Au-WO_{3-x} composite films depend very much on their microstructures as shown in Figure 4 for 20° and 500°C films where the grain size of Au on both films are significantly different. Neither Maxwell-Garnett nor Bruggeman formulations above explicitly reveal the dependence of the effective dielectric constant on grain sizes and shapes, and their applicability is typically restricted to situation when grain size is much smaller than the wavelength of the incident radiation at which Rayleigh theory of scattering is applicable. Under such conditions, the particles scatter radiation weakly and essentially behave as electric dipoles under the action of the electromagnetic fields. However, as shown in the insert of Figure 4, even the grain size of Au in the 500°C film (i.e. ~60 nm) is still much smaller than the wavelength of the incident radiation (i.e. 640 nm), the experimental SPR response for this 500°C film is much more derivate from theoretical simulation than that of the 20°C film where the grain size of both Au and WO_{3-x} are much smaller. This result indicates that the applicable range of both Maxwell-Garnett and Bruggeman formulations is smaller than what is suggested. When grain size even becomes bigger and comparable to the wavelength of the incident radiation, metallic particles will produce a considerable amount of multiple scattering, it is expected that theoretical simulation will even more derivate from experimental data. In addition, both Maxwell-Garnett and Bruggeman theories which assumes metallic particles are spherical can not explain the observed dielectric function anisotropy for composite with large ellipsoidal particles. Numerous models that have been developed to account for larger particles sizes [20] and for metal concentrations close to percolation conditions [16], [17] should be used.

4. Conclusions

SPR responses of Au-WO_{3-x} nanocomposite films were measured and calculated for various metal percentages and film thicknesses in the Kretschmann configuration. As the metal volume percentages in the composite thin films decrease, the reflectance minima of the SPR response shift to larger incident angle, and the width of the SPR dip became broader and broader. When the Au percentage reached 75%, the reflectance minimum of the SPR response became undistinguishable, i.e. no clear dip in the SPR response. Both the width and reflectance value at minima of the SPR dip depend on the thickness of the films. The SPR response of composite films was simulated using either Bruggeman or Maxwell-Garnett formulation with Macleod's general characteristic matrices method. The theoretical calculation based on the two models did not precisely fit the experimental data indicating that using a simple effective dielectric constant calculated with effective-medium theories to explain optical properties of such inhomogeneous materials is rather limited. However, the theoretical simulation is able to predict the trend in term of the dependence of SPR responses of Au-WO_{3-x} composite films on Au content and film thickness.

Acknowledgements

This work was supported under jointed NRC-NSC-ITRI (Canada-Taiwan) Nanotechnology Initiatives. Dr. B. Chen would also like to thank the Natural Science and Engineering Research Council of Canada for providing her with the postdoctoral fellowship. The authors are also indebted to Dr. S. Lee, Mr. H. Reshef, and Mr. M. Meinert of the NRC-IMI for their technical assistant.

References

[1]. A. Otto, *"Excitation of nonradiative surface plasma waves in silver by the method of frustrated total reflection"*, Zeitschrift fur Physik, 216:398–410, August 1968.

[2]. Erwin Kretschmann and Heinz Raether, "Radiative decay of non-radiative surface plasmons excited by light", Zeitschrift Fur Naturforschung, 23A:2135–2136, 1968.

[3] S. R. Emory, and S. Nie, *"Probing single molecules and single nanoparticles by surface-enhanced Raman scattering,"* Science 275, 1102-6, (1997).

[4] C. E. H. Berger, T. A. M. Beumer, R. P. H. Kooyman, and J. Greve, *"Surface Plasmon resonance multisensing,"* Anal. Chem. 70, 703-6, (1998).

[5] C. R. Yonzon, D. A. Stuart, X. Zhang, A. D. McFarland, C. L. Haynes, R. P. Van Duyne, *"Towards advanced chemical and biological nanosensors: an overview"*, Talanta 67, 438-48, (2005).

[6] Paras N. Prasad, *"Nanophotonics"*, Wiley-Interscience, 2004.

[7] G. A. Niklasson, C. G. Granqvist, and O. Hunderi, "*Effective medium models for the optical properties of inhomogeneous materials*", Applied Optics, 20(1):26–30, 1981.

[8] W. P. Chen and J. M. Chen, *"Use of surface plasma waves for determination of the thickness and optical constants of thin metallic films"*, J. Opt. Soc. Am., 71(2):189–191, February 1981.

[9] L. G. Schulz, *"The optical constants of silver, gold, copper, and aluminum, I, the absorption coefficient k"*, J. Opt. Soc. Am., 44(5):357–362, May 1954.

[10] H. Angus Macleod, "*Thin Film Optical Filters*", Institute of Physics Publishing, Bristol and Philadelphia, 3rd edition, 2001.

[11] *K.* S. Patel and H. T. Sun, *"Ceramic semiconductors for gas detection"*, Key Engineering Materials, 115:181–190, 1996.

[12] M. Penza, G. Cassano, and F. Tortorella, *"Gas recognition by activated WO_3 thin-film sensors array"*, Sensors and Actuators B, 81:115–121, 2001.

[13] J. R. Sambles, G. W. Bradbery, and Fuzi Yang, *"Optical excitation of surface plasmons: an introduction"*, Contemporary Physics, 32(3):173–183, 1991.

[14] S. Boughaba, G. I. Sproule, J. P. McCaffrey, M. Islam and M. J. Graham, *"Synthesis of tantalum pentoxide films by pulsed laser deposition: material characterization and scale-up"*, Thin Solid Films 358 (2000) 104-113.

[15] J. R. Sambles, G. W. Bradbery, and Fuzi Yang, *"Optical excitation of surface plasmons: an introduction"*, Contemporary Physics, 32(3):173–183, 1991.

[16] David R. Lide, editor, "*CRC Handbook of Chemistry and Physics*", CRC Press, 87th edition, June 2006.

[17] Edward D. Palik, editor, *"Handbook of Optical Constants of Solids"*, Academic Press, 1998.

[18] Henghua Denga, Dongfang Yang, Bo Chen, Chii-Wann Lin, "Simulation of surface plasmon resonance of Au–WO_{3-x} and Ag–WO_{3-x} nanocomposite films", Sensors and Actuators B 134 (2008) 502–509.

[19] Douglas B. Chrisey and Graham K. Hubler, editors, *"Pulsed Laser Deposition of Thin Films"*, Wiley-Interscience, 1994.

[20] Cheng-Chung Lee and Yi-Jun Jen, *"Influence of surface roughness on the calculation of optical constants of a metallic film by attenuated total reflection"*, Applied Optics, 38(28):6029–6033, October 1999.

Figure Captions

Figure 1: SPR responses of Au-WO_{3-x} composite films with various Au volume percentages. Solid line corresponds to experimental data, while the dashed line to simulation results.

Figure 2: SPR responses of Au-WO_{3-x} composite films with 88 value % Au of various film thicknesses. Solid line corresponds to experimental data, while the dashed line to simulation results.

Figure 3: Experimental SPR response of a 45 nm 91 % Au-WO_{3-x} films as comparing to theoretical simulation using both Maxwell-Garmet and Bruggeman theories for the effective dielectric constant calculation.

Figure 4: SPR response of Au-WO_{3-x} composite films with 88 % Au volume percentage deposited at 20°C and 500°C substrate temperatures, respectively. The inset corresponds to the FESEM images of the film surfaces.

Figure 5: X-ray diffraction patterns for the Au-WO_{3-x} composite films deposited on BK7 substrates at 20°C and 500°C substrate temperatures, respectively.

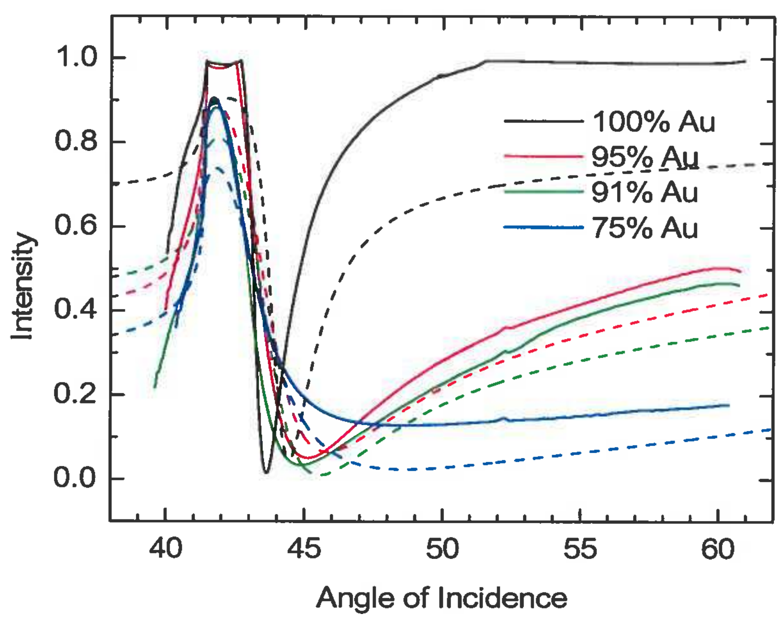

Fig. 1

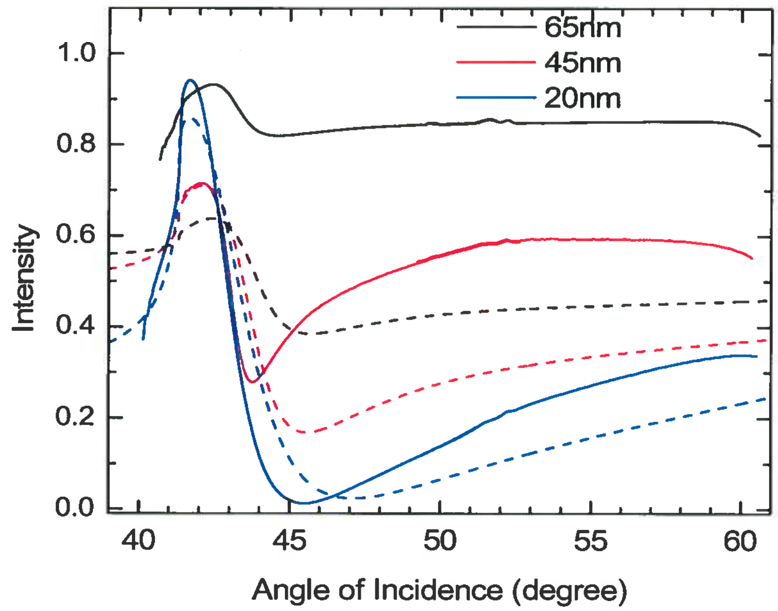
65nm
45nm
20nm
1.0
0.8
0.6
0.4
0.2
0.0
Intensity
40
45
50
55
60
Angle of Incidence (degree)

Fig. 2

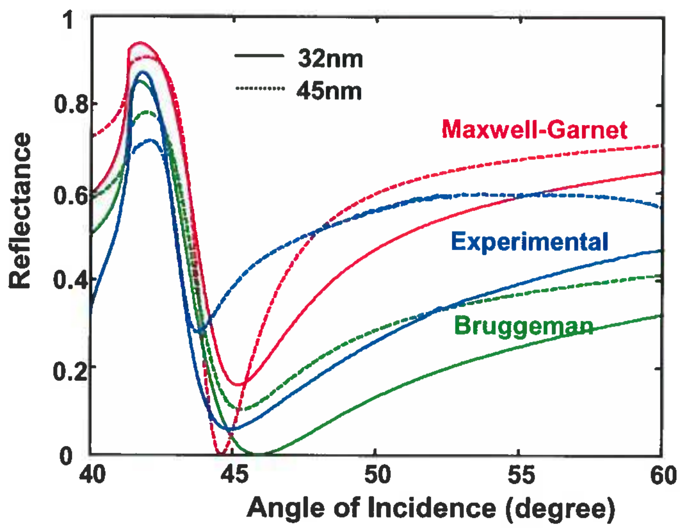
32nm
45nm
Maxwell-Garnet
Experimental
Bruggeman
Reflectance
Angle of Incidence (degree)
1
0.8
0.6
0.4
0.2
0
40
45
50
55
60

Fig. 3

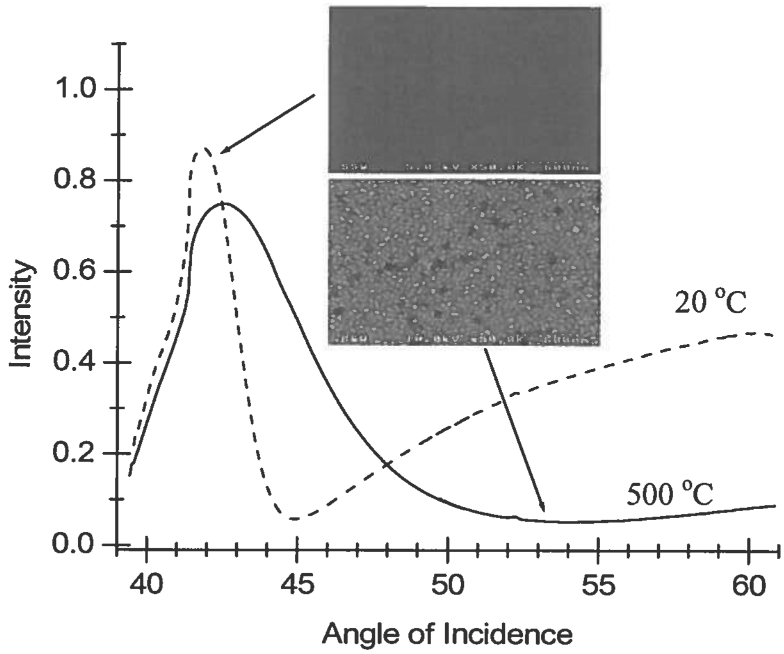
1.0
0.8
0.6
0.4
0.2
0.0
Intensity
40
45
50
55
60
Angle of Incidence
20 °C
500 °C

Fig. 4

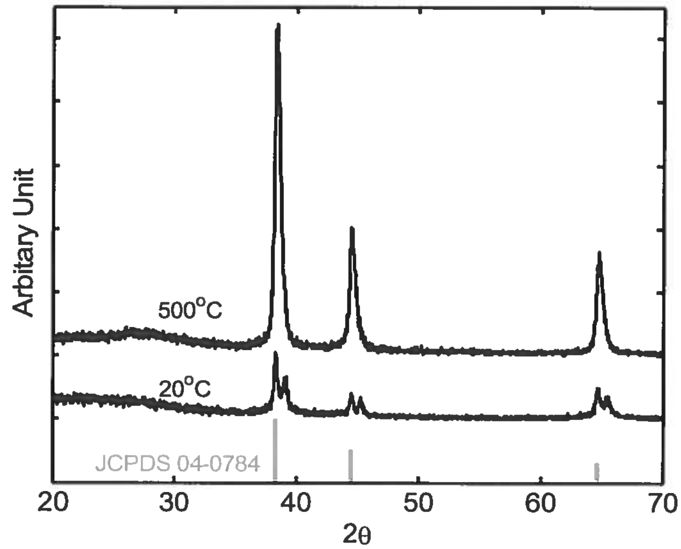

Fig. 5